Precipitation modification by ionization

Article

Accepted Version

Harrison, R. G., Nicoll, K. A., Ambaum, M. H. P., Marlton, G. J., Aplin, K. L. and Lockwood, M. (2020) Precipitation modification by ionization. Physical Review Letters, 124 (19). 198701. ISSN 0031-9007 doi: https://doi.org/10.1103/PhysRevLett.124.198701 Available at https://centaur.reading.ac.uk/90278/

Precipitation modification by ionisation

R. Giles Harrison[1], Keri A. Nicoll[1,2], Maarten H.P. Ambaum[1], Graeme J. Marlton[1], Karen L. Aplin[3], Michael Lockwood[1]

[1]*Department of Meteorology, University of Reading, UK*
[2]*Department of Electronic and Electrical Engineering, University of Bath, UK*
[3]*Aerospace Engineering, University of Bristol, UK*

Forthcoming in *Physical Review Letters* (LM16559)

Abstract

Rainfall is hypothesised to be influenced by droplet charge, which is related to the global circuit current flowing through clouds. This is tested through examining a major global circuit current increase following release of artificial radioactivity. Significant changes occurred in daily rainfall distribution in the Shetland Islands, away from pollution. Daily rainfall changed by 24%, and local cloud optically thickened, within the nuclear weapons test period. This supports expectations of electrically induced microphysical changes in liquid water clouds from additional ionisation.

Keywords: atmospheric electricity; radioactivity; nuclear explosion; geoengineering

1. Introduction

Rain production in warm clouds depends on rapid growth of small droplets, through condensation, collision and coalescence, until the drops are large enough to fall to the surface. For charged droplets, their collision efficiencies are modified by electrical forces, which may influence clouds and ultimately affect precipitation [1,2]. Droplet charging results from aerosol or ions transferring their charge to the droplets on collision, or self-generation of charge from radioactive decay [3]. In persistent extensive layer clouds, droplet charging occurs from global circuit current flow through the cloud. An important property of water droplets is their polarisability, causing image charge interactions. This means that, at small separations, the electric force between charged droplets is always attractive, independent of net polarity [4].

Appreciable modification of droplet charge is required for electrical effects on precipitation to be detectable, for example through an increased global circuit current. Solar effects provide one route [5], but solar cycle changes in conduction current are small. An alternative approach is pursued here, by examining data from the period of nuclear weapons tests in the late 1950s and early 1960s, which injected substantial radioactivity into the stratosphere globally [6,7]. (See also Figure S1). Downwards transport of radioactive material by sedimentation and wet removal generated increased lower atmosphere (tropospheric) ionisation. Such extreme changes, causing unusual electrical disturbances over a wide area, are important because they are never likely to be achieved by planned experimental means [8]. Here, new insights from combining datasets of atmospheric electricity and meteorological quantities are considered further.

2. Observations of atmospheric electrical effects of radioactivity

Release of radioactivity to the atmosphere increases the air conductivity through ionisation. If radioactivity is deposited on the surface, the atmospheric electric field magnitude can be greatly

reduced, as observed after the Chernobyl [9] and Fukushima disasters [10]. This was first noticed following radioactive deposition from the nuclear weapons tests in the 1950s and early 1960s [11] through multiple stations globally showing a common reduction in the Potential Gradient (PG) [12].

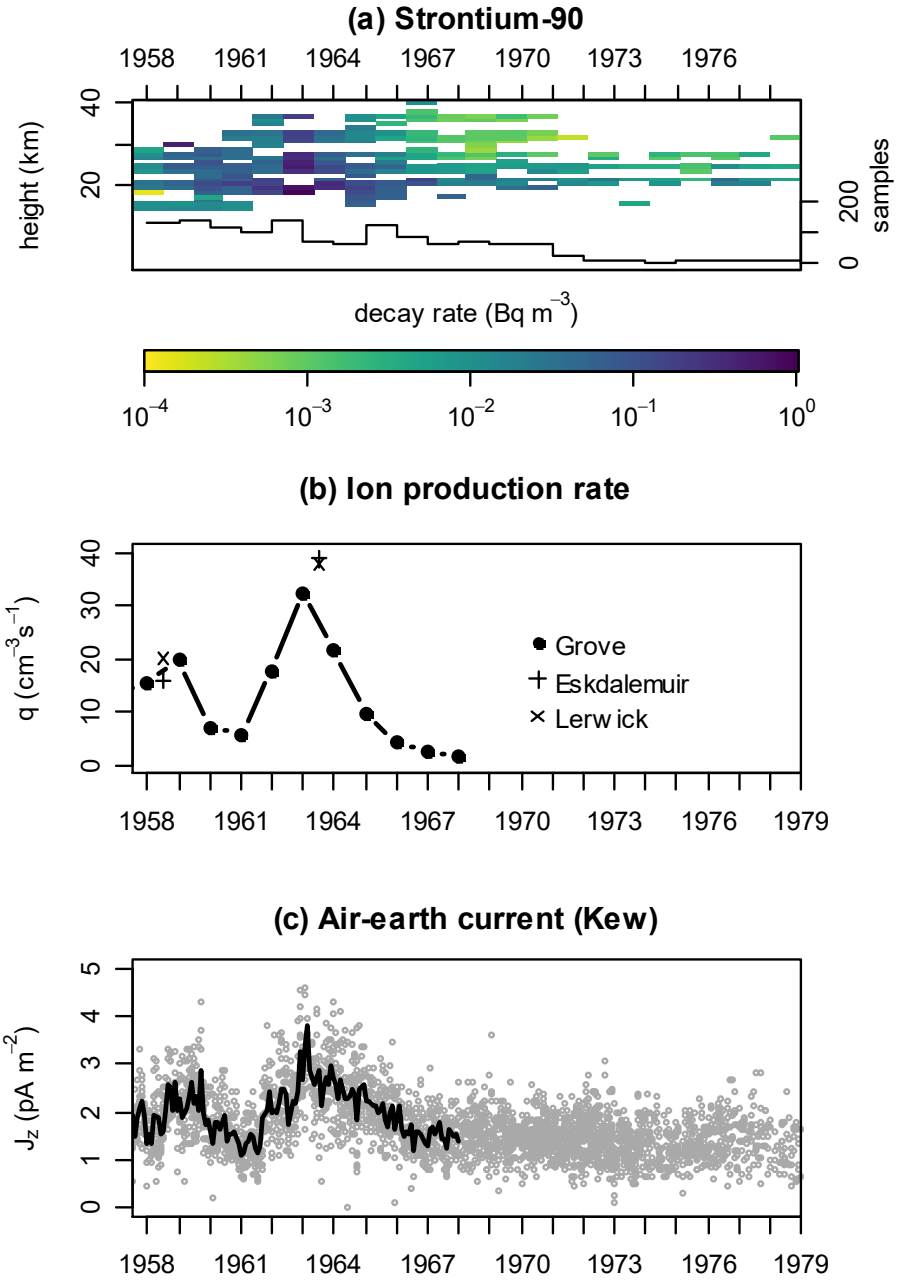

Figure 1. (a) Stratospheric ^{90}Sr decay measurements from the High Altitude Sampling Program (in becquerels per standard m^3 of air) for the northern hemisphere (averaged between 22.5°N to 65°N, showing annual number of samples). (b) Surface (the lowest metre) ion production rate *q* at the UK sites of Grove, Oxfordshire (points), Eskdalemuir, Scotland (cross-hairs) and Lerwick, Shetland (crosses). (c) Vertical air-earth current density J_z on fair weather days at Kew Observatory, London, at 15UTC. The solid black line shows monthly mean values.

Further analysis of ionisation effects on atmospheric processes is facilitated by data now widely available, for example radioactivity sampling from the High Altitude Sampling Program (HASP), which collected fission debris on paper filters for analysis. Atmospheric Strontium-90 became the principal focus of HASP, and annual average ^{90}Sr concentrations from the northern hemisphere are presented in figure 1a. Figure 1b shows the near-surface ion production rate q measured by routine monitoring at sites across the UK at Grove (51°30'N, 1°W), Eskdalemuir (55°19'N, 3°12'W) and Lerwick (60°09'N, 1°08'W), in which q increases simultaneously with atmospheric Sr-90 in 1962-64 [13],[14]. Finally, figure 1c shows that the vertical current density at Kew, near London (51°28'N, 0°19'W), also increased. (Table S1 summarises the Kew atmospheric electricity data). Specifically, median J_z at Kew for 1962-64 was 2.5 pA m^{-2}, with a 99th percentile of 4.6 pA m^{-2}; for the more settled period 1966-71 the median J_z was 1.52 pA m^{-2}, with 99th percentile of 2.5 pA m^{-2}. The increase in median J_z 1962-64 over 1966-71 was therefore 63%, and on some days transiently much more. (Figure S2 shows the sites' locations).

At Kew, vertical current density J_z was measured using the manual Wilson plate method [15]. This provided independent measurements of PG and J_z around 15 UTC daily when the weather was fine (i.e. without precipitation), by repeated exposure and covering of a sensing plate connected to an electrometer, with air conductivity derived by Ohm's Law [16]. Whilst the PG was reduced at Kew during 1962-64, it did not show as a dramatic reduction at Eskdalemuir and Lerwick during the 1960s [12]. This could be related to different operating principles (electrostatic induction at Kew rather than a collecting probe at Eskdalemuir and Lerwick), or the protection provided by the cover plate. Lack of a catastrophic reduction in the Kew PG suggests the site avoided significant surface radioactive contamination, possibly related to the substantial smoke pollution in London [11]. The Wilson apparatus was rebuilt in the early 1950s following acid rain damage, fully functional by July 1956 [16, 17].

3. Quantitative estimates of atmospheric electricity effects

Adding radioactivity to air increases ion production, and, in turn, the air conductivity σ. The increased conductivity will reduce the resistance of a unit area column of air above, *i.e*. the columnar resistance, R_c, depending on the vertical distribution of additional radioactive ionisation. R_c is given by integrating σ with height z, as

$$R_c = \int_0^{z_u} \frac{dz}{\sigma(z)} \tag{1}$$

where negligible further resistance is contributed above z_u. At Kew during 1969-1971, after the effects of weapons testing had diminished, R_c varied between 64 PΩ m^2 and 210 PΩ m^2, with a median of 145 PΩ m^2 [18]. σ is given by

$$\sigma = 2n\mu e \tag{2}$$

for air containing equal number concentrations of bipolar ions n with mean mobility μ, and e the elementary charge. Ion removal has two limiting conditions for clean and polluted air [19]. In polluted urban air, ion removal is dominated by ion-aerosol attachment. n is accordingly proportional to the ion production rate, and inversely proportional to the aerosol particle number concentration Z and ion-aerosol loss coefficient β, which depends on particle size and charge. In this limit, σ at the same height is described by

$$\sigma = 2\frac{(q_b+q_r)}{\beta Z}\mu e \tag{3}.$$

where q_b is the volumetric background ion production rate and q_r any additional radioactive ionisation [19]. For 1962-1964, the median surface conductivity σ_s (*i.e.* $\sigma(0)$ in equation (1)) was 10 fS m^{-1} at Kew,

compared with 4.6 fS m^{-1} for 1966-1971, indicating $q_r \approx q_b$, and, from equation (3), a doubling of the ion concentration in surface air.

Variability in R_c above Kew can be approximated from surface measurements by combining a lower polluted layer contribution R_{PL} and a fixed upper "free troposphere" term R_{FT} [20]. If the lower layer is represented by a depth k, R_{PL} can be found from the surface conductivity as k/σ_s. This gives

$$R_c = \frac{k}{\sigma_s} + R_{FT} \quad (4),$$

with R_{FT} = (93 ±18) PΩ m^2 and k = (270±90) m. The 1962-1964 increase in median σ_s at Kew therefore indicates a halving of the lower part of the columnar resistance. The effect on the upper resistance can be estimated from the radioactive decay rate, as, in the other limiting condition of clean air, ion removal occurs through ion-ion recombination: n is hence proportional to the square root of the ion production rate [19]. For radioactive air generating decay products at a rate η per unit volume of average energy E_{av}, the radioactive ion production rate q_r is

$$q_r = \eta \frac{E_{av}}{w_i} \quad (5),$$

with w_i the mean ionisation energy in air, ~35 eV [21]. Assuming beta emission of ^{90}Sr dominated the atmospheric ionisation, for which E_{av} = 196 keV [22], equation (5) gives ion production rate from ^{90}Sr as $q_r = 5600\ \eta_{Sr90}$, for η_{Sr90} the decay rate of ^{90}Sr. The background ion production rate in the troposphere at 10 km is $q_b \approx 10^7$ m^{-3} [23], which indicates that $\eta_{Sr90} \geq 1800$ Bq m^{-3} is required for the ionisation rate to double and hence the lower atmosphere dominates.

Halving the lower atmosphere contribution (estimated from assuming the maximum R_c of [18] would best represent the more polluted conditions earlier in the decade), R_c would be reduced from 210 PΩ m^2 to 152 PΩ m^2, i.e. by a factor of ~0.7. Assuming a steady ionospheric potential, this R_c change would account for the approximate doubling of J_z observed at Kew. This is conservative, as if the ionospheric potential also increased as seems likely [24, 25], this would increase J_z further by about 50%.

4. Effects on clouds and precipitation

The electrical observations, surface ionisation and enhanced stratospheric ^{90}Sr of figure 1 clearly demonstrate that additional atmospheric ionisation was present during 1962-64, leading to an increase in the global circuit's conduction current. The stratospheric radioactive material was so extensively distributed in the northern hemisphere (e.g. figure S3), that similar electrical changes are expected widely. (The 1962-64 HASP data is dominated by 30°N samples, hence the 51°N response at Kew demonstrates this). This section considers whether effects of the disturbed conditions can be detected in cloud and precipitation data from Lerwick Observatory in Shetland. Lerwick is distant from urban air pollution, and PG was measured at the time of interest [26]. Evidence of increased air conductivity above Lerwick comes from the profound reduction in PG during 1962-1964, with a recovery from 1964-1966 (figure 2a). This resulted from surface radioactive contamination from above, through rainfall or dry deposition, which would increase the near-surface air conductivity.

(a) Cloud data

Observers can identify cloud type and estimate coverage, but cannot provide precise determination of cloud amount and thickness, nor sensitivity to subtle changes. Objective cloud information during daylight hours can be inferred from automatic measurements of solar radiation on a horizontal surface, using the global solar irradiance S_g (i.e. total direct and scattered diffuse radiation) and diffuse solar irradiance S_d, measured hourly at Lerwick from 1952. Two cloud-related quantities can be derived from S_d and S_g [27]. The *diffuse fraction* (DF) is given by

$$DF = \frac{S_d}{S_g} \quad (6).$$

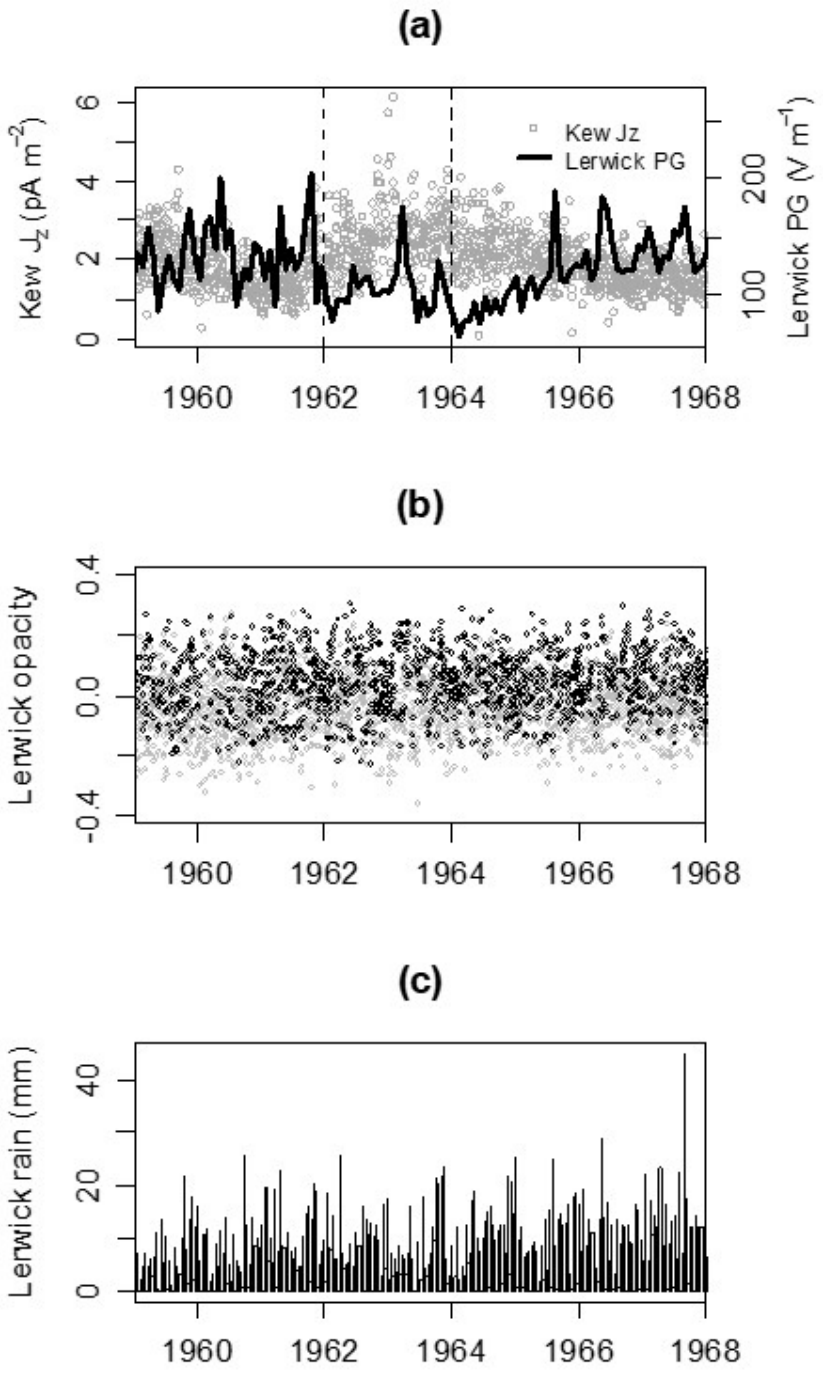

Figure 2. (a) Time series of air-earth current density J_z at Kew Observatory on fair weather days (points) and fair weather Potential Gradient (PG, solid line from monthly values) at Lerwick Observatory, Shetland. (b) Time series of seasonally detrended daily cloud optical thickness at Lerwick (from the ratio of hourly measured solar radiation to the calculated top of atmosphere solar irradiance, for horizontal surfaces). Overcast days (defined as mean daily diffuse fraction >0.9) are shown as black points. (Daily values from 1956 to 1979 were used to determine the seasonal variation, which was subtracted). (c) Daily rainfall totals at Lerwick between 09 and 21 UTC.

Absolute values of *DF* vary from ~0.2 in clear conditions, to 0.9 or greater when the sky is fully overcast: this allows *DF* to signify overcast conditions. A second measure of cloud coverage (Opaqueness *Op*) is provided by the ratio of the horizontally-incident surface radiation to that expected at the top of the atmosphere, as

$$Op = 1 - \frac{S_g}{S_{TOA}} \quad (7),$$

where S_{TOA} is the calculated astronomical top of atmosphere solar irradiance. *Op* varies from about 0.2 in clear conditions to about 0.95 under thick cloud and is correlated with *DF* in broken cloud [27]. By combining *DF* and *Op*, the *DF* threshold of 0.9 can identify overcast conditions, whilst *Op* provides a measure of overcast opacity. The Lerwick hourly S_d and S_g are used to calculate daily values of *DF* and *Op* (figure S4). The mean seasonal variation for *Op* is also calculated, which is subtracted to give anomalies from the mean: positive anomalies therefore indicate values greater than the seasonal mean (i.e. thicker cloud), and negative anomalies values less than the seasonal mean. Figure 2b shows the time series of seasonally-detrended *Op*, on which overcast days (from the *DF* criterion) which are frequent at Lerwick, are marked.

(b) Rainfall data

Lerwick Observatory reported daily rainfall using a standard rain gauge, emptied at 09 UTC and 21 UTC. The rainfall totals at 21 UTC, i.e. rainfall for the 12 hours from 09 to 21 UTC, are used here (presented as a time series in figure 2c), as they are will include daylight allowing comparison with cloud data from solar radiation, and span the 15 UTC measurement of J_z at Kew.

5. Analysis

Daily cloud and rainfall data from Lerwick are compared with Kew J_z data, assuming the current density passing through cloud at Lerwick was similarly affected to Kew. This is justified by the extensive radioactivity observed above both sites (figure S3). From figure 1 and figure 2a, 1962-64 are strongly disturbed, hence the analysis is for this period. A later undisturbed period is provided for comparison.

Firstly, cloud opacity anomalies on overcast days 1962-64 are compared with the rainfall on the same days (figure 3a). It is immediately apparent that optically thicker clouds are associated with greater rainfall, with an odds ratio from dividing the data at the median of 3.21 ($p<10^{-4}$). In Figure 3b, the Lerwick overcast opacity data is plotted against the Kew J_z data. (Note that there are fewer days than for figure 3a, as fine days were required at Kew, 600 miles distant, for the J_z measurements). If the Lerwick *Op* data values are divided into the lower and upper quartiles of Kew J_z (i.e. when $J_z < 2$pA m^{-2} giving 37 points and $J_z > 2.93$ pA m^{-2} giving 34 points), the two clusters of points from Lerwick show some differences: more values of greater opacity occur for the upper J_z values compared with the lower J_z. The medians of the opacity anomalies for the lower and upper current densities are *Op*=0.026 and *Op*=0.082, with the distributions significantly different (p=0.025) using a Mann-Whitney test.

The relationship between overcast day opacity and rainfall in figure 3a indicates a possible effect of electrically disturbed conditions on precipitation. A similar approach has therefore been taken to investigate daily rainfall data (figure 3c), i.e. by splitting it according to the daily Kew J_z, in this case at the median (J_z=2.5 pA m^{-2}). The groups of points again differ in character between the lower and upper halves, with the lower J_z points clustering around lower rainfalls. For the 76 days with lower J_z and the 61 days with greater J_z the aggregated rainfalls are very similar (158.5 mm and 156 mm respectively), but, as the rainfall occurs on fewer days in the latter case, this represents a shift from 2.1 mm to 2.6 mm of daily rain. This 24% increase in daily rain accompanies a 47% increase in current density

from 2 pA m^{-2} to 2.9 pA m^{-2}, using the quartile values to represent the upper and lower currents either side of the median. A Kolmogorov-Smirnov (K-S) test to assess whether the two distributions are different rejects the null hypothesis that the values are drawn from the same distribution (p=0.04). Figure 3d shows the disturbed period Lerwick rainfall data as overlain probability density distributions. For rainfall associated with greater J_z, the rainfall distribution shifts towards larger values.

The cumulative distribution functions underlying the K-S test are shown for the radioactively disturbed period (figures 3e), and a later undisturbed period (figure 3f). In the disturbed period, daily rainfall amounts exceeding 4 mm occur more frequently for greater J_z than lesser J_z, with lighter rain events less common. Applying the same separation methodology for data from the later undisturbed period, the two distributions were not found significantly different by the K-S test.

6. Discussion

Enhanced tropospheric radioactivity could influence the electrical properties of clouds in different ways. Firstly, an ionisation-associated increase in the conduction current density, due to a regionally reduced columnar resistance, would lead to increased cloud droplet charging at the horizontal boundary of layer clouds [2, 28]. Secondly, if radioactive aerosol is present, it could be preferentially removed by water droplets, transferring charge to them [3, 29]. In either case, modelling [2] suggests that production of raindrops would be encouraged by charge on small cloud droplets, and that only ~10e per droplet is needed to influence droplet-droplet collisions through the image force.

This analysis of the Lerwick data in terms of J_z changes during spatially-extensive disturbed conditions generated by the nuclear weapons tests shows, both, that cloud properties changed significantly toward thicker clouds in this period, and, on rainfall days, that daily precipitation amounts were greater (by 24%). Whilst the mechanism cannot be precisely identified, the responses observed are not inconsistent with charge-induced microphysical changes, such as from an increased conduction current density. This supports expectations of electrically induced effects in liquid water clouds from additional ionisation.

The atmospheric conditions of 1962-64 were exceptional and it is unlikely they will be repeated, for many reasons. An alternative, safer, method of artificially increasing local ionisation is to employ corona ion emission. To influence clouds the ionisation would need to be delivered by aircraft, over a sufficient volume to, at least, double the ion concentration (section 3). As corona ionisation leaves no residue and is short-lived in its effects, it may therefore be promising for local rainfall modification or even geoengineering of cloud properties.

Acknowledgements: RGH, KAN, GJM and MHPA are supported through the UAE Rain Enhancement Programme's project "Electrical aspects of rainfall generation". KAN also acknowledges NERC support through Independent Research Fellowships (NE/L011514/1 and NE/L011514/2). The Met Office originally made the atmospheric electrical measurements at Kew and Lerwick Observatories, which were transcribed for analysis from the Observatories' Yearbook for the years concerned; the Lerwick meteorological data was from the Met Office Integrated Data Archive System (MIDAS) from the CEDA repository http://catalogue.ceda.ac.uk/uuid/220a65615218d5c9cc9e4785a3234bd0. HASP data was obtained from the Environmental Measurements Laboratory (https://www.wipp.energy.gov/NAMP/EMLLegacy/databases.htm).

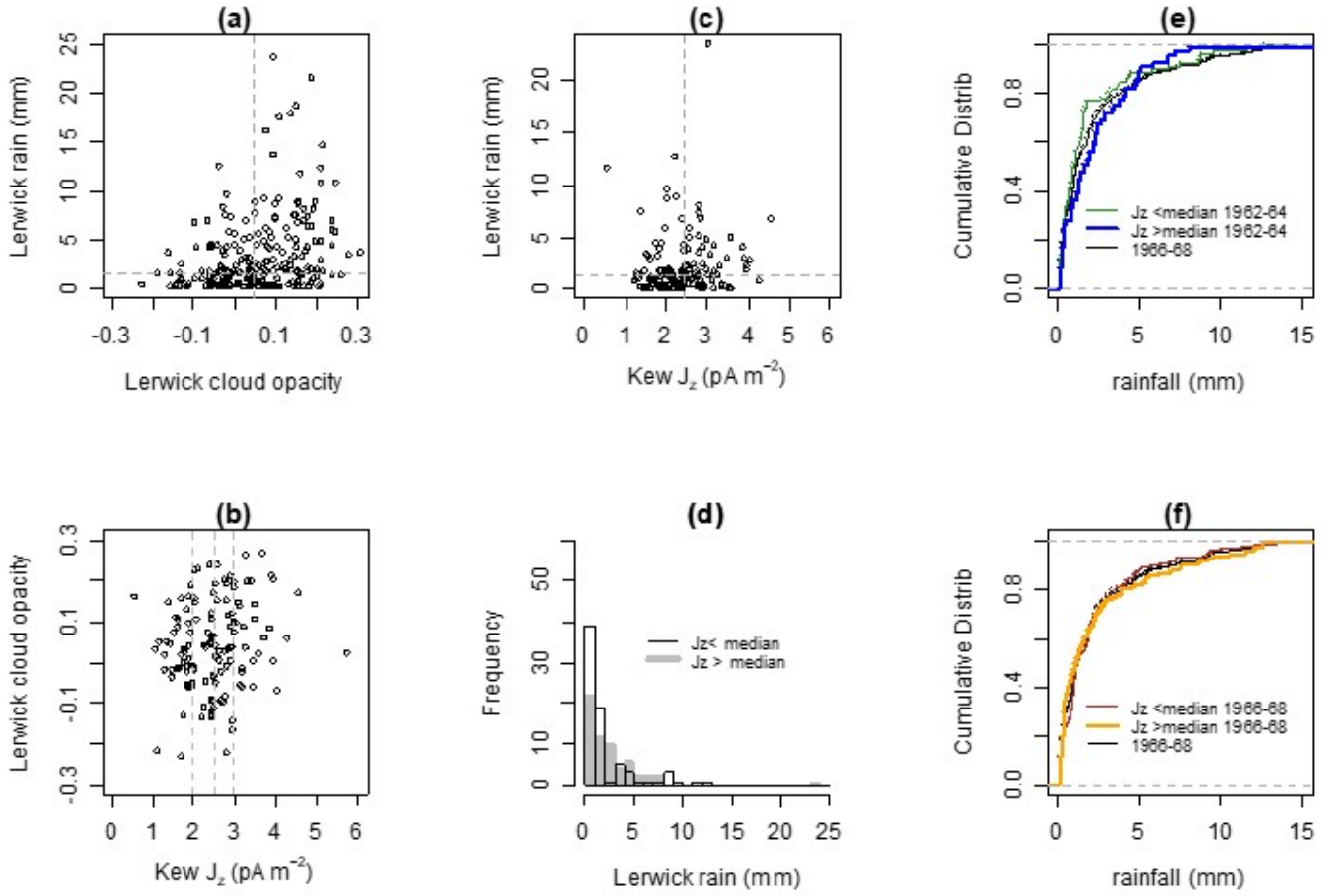

Figure 3. Daily cloud and rainfall at Lerwick compared with Kew J_z data. Seasonally-detrended cloud opacity at Lerwick 1962-64 plotted against (a) Lerwick rainfall (216 days) and (b) Kew air-earth current density J_z (137 days), with the medians marked with dashed lines. Daily rainfall at Lerwick 1962-1964, (c) plotted against Kew J_z, with the median marked (grey dashed line), and (d) divided by when the Kew J_z was above and below its median value (1962-1964) of 2.5 pA m^{-2}. Normalised cumulative distributions for rain days for (e) the disturbed period 1962-1964 and (f) undisturbed period 1966-1968, divided by when Kew J_z was above (thick lines) and below (thin lines) its median. The cumulative density function for rain days 1966-1968 is also shown (black line).

References

[1] A. Khain, V. Arkhipov, M. Pinsky, Y. Feldman, Y. Ryabov, Rain enhancement and fog elimination by seeding with charged droplets. part I: Theory and numerical simulations. *J Appl. Met* **43**, 1513-1529 (2004)

[2] R.G. Harrison, K.A. Nicoll, M.H.P. Ambaum, On the microphysical effects of observed cloud edge charging *Quart J Roy Meteorol Soc* 141, 2690-2699, doi: 10.1002/qj.2554 (2015)

[3] C.F. Clement and R.G. Harrison, The charging of radioactive aerosols *J. Aerosol Sci* **23**, 5, 481-504 (1992)

[4] J. Lekner, Electrostatics of two charged conducting spheres. *Proc. R. Soc. London* A 471: 2174, doi: 10.1098/rspa.2012.0133 (2012)

[5] K.A. Nicoll and R.G. Harrison, Detection of lower tropospheric responses to solar energetic particles at mid-latitudes *Phys Rev Lett* **112**, 225001 (2014)

[6] F. Warner and R.J.C. Kirchmann, Nuclear test explosions - Environmental and Human Impacts (Scientific Committee on Problems of the Environment, 59), Wiley (2000)

[7] WMO, Meteorological aspects of atmospheric radioactivity. World Meteorological Organisation Technical Note 68 (WMO-No.169.TP.83), 194pp, Geneva (1965)

[8] R.G. Harrison, The global atmospheric electrical circuit and climate *Surv Geophys* 25, (5-6), 441-484, doi: 10.1007/s10712-004-5439-8 (2004)

[9] S. Warzecha, Results of atmospheric electricity measurements at Swider after the Chernobyl nuclear power plant accident *Publs Insts Geophys Pol Acad Sci* D-26 (198) (1987)

[10] M. Takeda, M. Yamauchi, M. Makino, and T. Owada, Initial effect of the Fukushima accident on atmospheric electricity *Geophys Res Lett* 38, L15811,doi:10.1029/2011GL048511 (2011)

[11] K.H. Stewart, Some recent changes in atmospheric electricity and their causes. *Quart J Roy Meteorol Soc* **86**, 369, 399-405 (1960)

[12] E.T. Pierce Radioactive fallout and secular effects in atmospheric electricity *J.Geophys. Res*. 77, 1, 482-487 (1972)

[13] J.A.B. Gibson, J.E. Richards and J. Docherty, Nuclear radiation in the environment - beta and gamma-ray dose rates and air ionisation from 1951 to 1968. *J Atmos Terr Phys* **31**, 1183-1196 (1969)

[14] R.A. Hamilton and J.G. Paren, The influence of radioactive fallout on the atmospheric potential gradient. *Meteorol Mag* **96**, 81-85 (1967)

[15] C.T.R. Wilson, On the measurement of the earth-air current and on the origin of atmospheric electricity. *Proc. Camb. Philos. Soc.* **13**, 6, 363-382 (1906)

[16] R.G. Harrison and W.J. Ingram, Air-earth current measurements at Kew, London, 1909-1979 *Atmos Res* **76**, (1-4), 49-64, doi:10.1016/j.atmosres.2004.11.022 (2005)

[17] R.G. Harrison, Urban smoke concentrations at Kew, London, 1898-2004 *Atmos Environ* **40**, 18, 3327-3332, doi: 10.1016/j.atmosenv.2006.01.042 (2006)

[18] M.J. Rycroft, R.G. Harrison, K.A. Nicoll and E.A. Mareev, An Overview of Earth's Global Electric Circuit and Atmospheric Conductivity *Space Science Reviews* **137**, 83-105 doi: 10.1007/s11214-008-9368-6 (2008)

[19] R.G. Harrison and K.S. Carslaw, Ion-aerosol-cloud processes in the lower atmosphere *Reviews of Geophysics* **41** (3), 1012, 10.1029/2002RG000114 (2003)

[20] R.G. Harrison and A.J. Bennett, Multi-station synthesis of early twentieth century surface atmospheric electricity measurements for upper tropospheric properties *Adv Geosci* **13**, 17-23 (2007)

[21] L. Christophorou, Atomic and molecular radiation physics Wiley, New York (1970)

[22] E. Browne, Nuclear Data Sheets for A=90. *Nucl Data Sheets* **82**, 379 (1997)

[23] G.A. Bazilevskaya, I.G. Usoskin, E.O. Flückiger, R.G. Harrison, L. Desorgher, R.B. Bütikofer, M.B. Krainev, V.S. Makhmutov, Y.I. Stozhkov, A.K. Svirzhevskaya, N.S. Svirzhevsky, G.A. Kovaltsov, Cosmic ray induced ion production in the atmosphere. *Space Science Reviews* **137***,* 149-173 doi: 10.1007/s11214-008-9339-y (2008)

[24] N.N. Slyunyaev, E.A. Mareev, and A.A. Zhidkov, On the variation of the ionospheric potential due to large-scale radioactivity enhancement and solar activity *J. Geophys. Res. Space Physics*, **120**, 7060–7082,doi:10.1002/2015JA021039 (2015)
[25] B.A. Tinsley, On the variability of the stratospheric column resistance in the global electric circuit *Atmos Res* **76**, 1-4, 78-94 (2005)
[26] R.G. Harrison and K.A. Nicoll**,** Air-earth current density measurements at Lerwick; implications for seasonality in the global electric circuit *Atmos Res* **89***,* 1-2, 181-193, doi:10.1016/j.atmosres.2008.01.008 (2008)
[27] R.G. Harrison, N. Chalmers, R.J. Hogan, Retrospective cloud determinations from surface solar radiation measurements *Atmos Res* **90**, 54-62.doi:10.1016/j.atmosres.2008.04.001 (2008)
[28] L. Zhou, and B.A. Tinsley, Production of space charge at the boundaries of layer clouds. *J Geophys Res: Atmospheres* **112**(D11) (2007)
[29] S.N. Tripathi and R.G. Harrison, Scavenging of electrified radioactive aerosol *Atmos Environ*, **35**, 33, 5817-5821 (2001)

Precipitation modification by ionisation

R. Giles Harrison[1], Keri A. Nicoll[1,2], Maarten H.P. Ambaum[1], Graeme J. Marlton[1], Karen L. Aplin[3], Michael Lockwood[1]

[1]*Department of Meteorology, University of Reading, UK*
[2]*Department of Electronic and Electrical Engineering, University of Bath, UK*
[3]*Aerospace Engineering, University of Bristol, UK*

Supplementary Information

This section provides additional information in support of the main text. It concerns the abundance and timing of atomic weapons test explosions (figure S1), a map of the sites discussed (figure S2), the distribution of atmospheric radioactivity observed (figure S3) and further details of the processing of the solar radiation data used in the analysis (figure S4). Table S1 provides a summary of the Kew atmospheric electricity data.

Figure S1

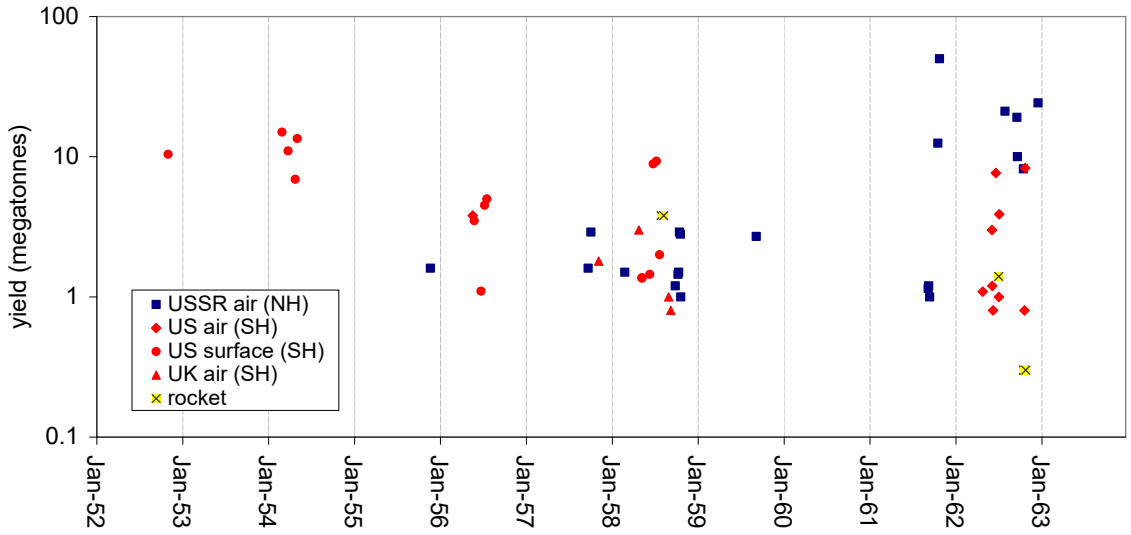

Figure S1. Time series of atomic weapon test explosions, for large yield events (>0.5 Megatonnes) in the northern or southern hemisphere (NH or SH), categorised by detonation environment (air, surface or rocket). (Compiled from [5])

Figure S2

Figure S2. Positions of the sites discussed: the geophysical observatories at Kew, Eskdalemuir and Lerwick, and the monitoring site at Grove.

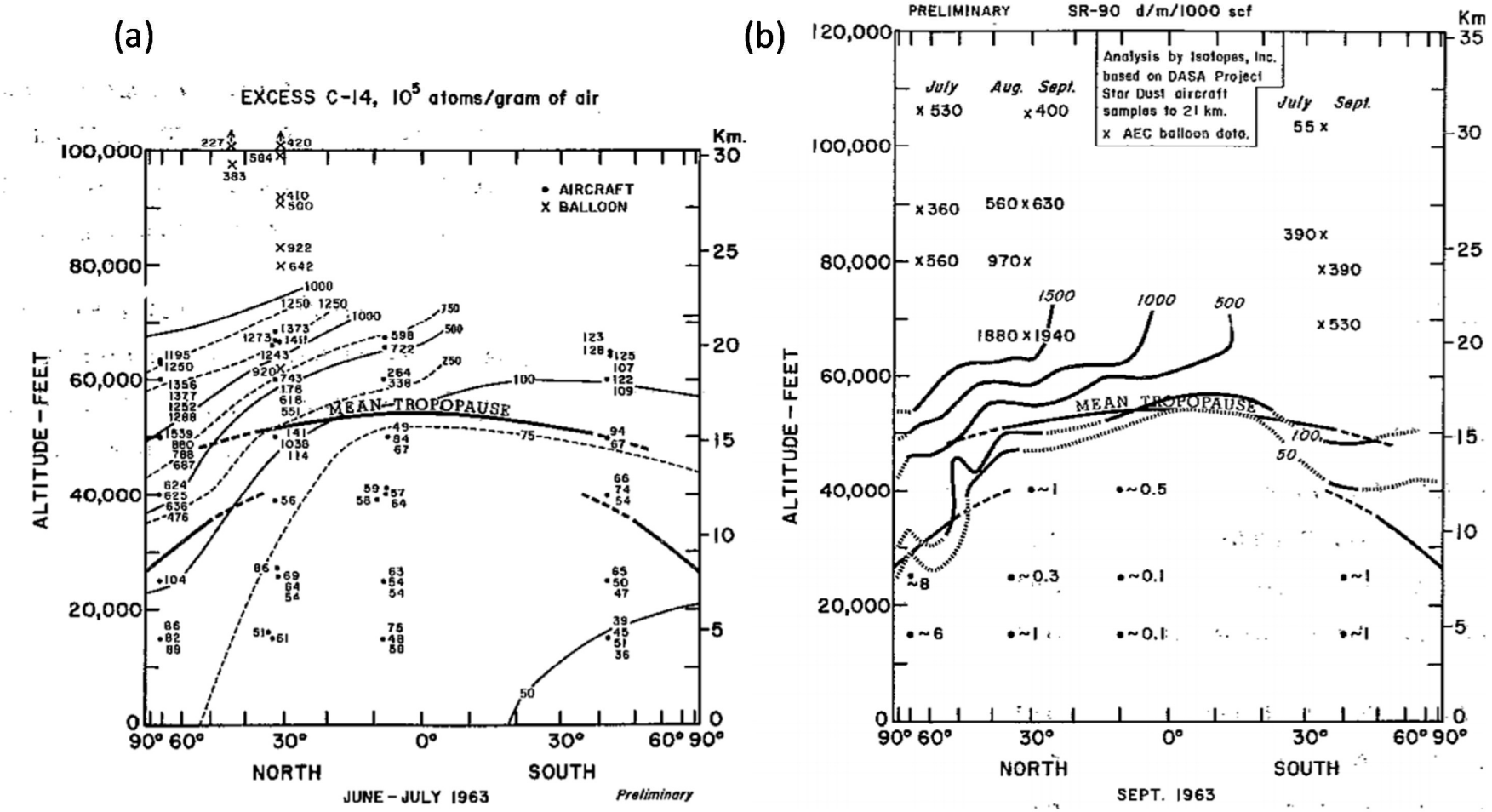

Figure S3. Pole to pole atmospheric cross section for (a) excess Carbon-14 in June-July 1963, and (b) Strontium-90 in September 1963. From *Meteorological aspects of atmospheric radioactivity* World Meteorological Organisation Technical Note 68 (WMO-No.169.TP.83), 194pp, Geneva (1965).

Figure S4

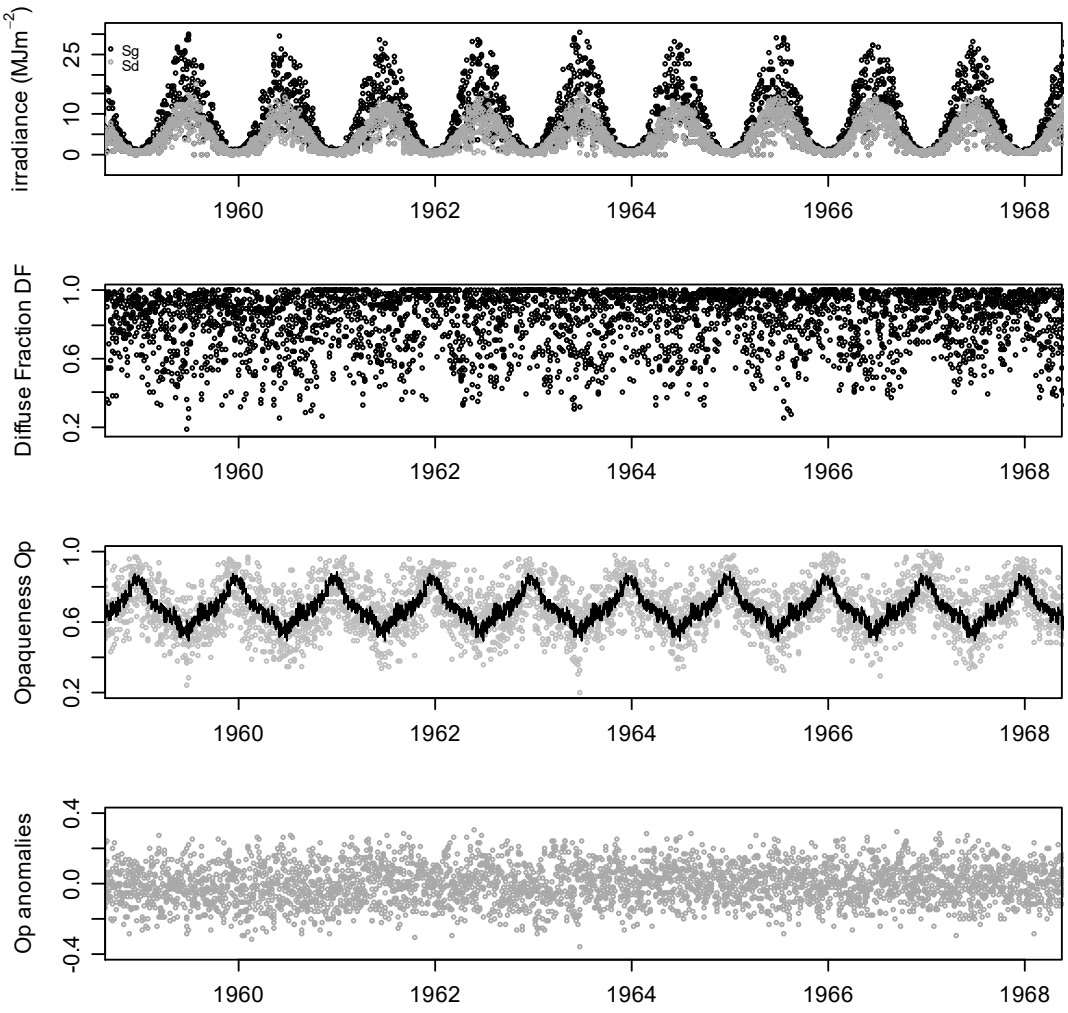

Figure S4. Surface solar radiation from Lerwick and derived quantities. (Top panel) Integrated measured daily global solar irradiance S_g and diffuse solar irradiance S_d. (Second panel) Daily diffuse fraction (DF), from S_d/S_g. (Third panel) Daily Opaqueness (1- S_g/S_{TOA}), where S_{TOA} is the calculated top of atmosphere solar irradiance. The average daily variation from 1956 to 1979 is shown by the black line. (Bottom panel). Daily anomalies in Opaqueness, found by subtracting the average variation on the same day from each daily value.

Table S1 - Summary of Kew atmospheric electricity data from the Wilson apparatus

Quantity	*statistic*	*1962-1964*	*1966-1971*
Current density J_z (pA m^{-2})	Lower quartile	2	1.27
	Median	2.48	1.52
	Upper quartile	2.93	1.77
Potential Gradient PG (V m^{-1})	Lower quartile	167	259
	Median	228	331
	Upper quartile	369	444
Conductivity σ (fS m^{-1})	Lower quartile	7.5	3.3
	Median	10	4.6
	Upper quartile	13.3	5.7